Assessment of Soil Erosion and Neotectonics Geomorphology of Bannu Basin using RS and GIS Techniques

Saira Batool[1], Syed Amer Mahmood[2], Zainab Tahir[1], Amer Masood[2], Jahanzeb Qureshi[2], Bushra Zia Khan[1], S M Hassan[2]
[1]Centre For Integrtaed Mountain Research(CIMR) University of the Punjab Lahore Pakistan
[2]Department of Space Science University of the Punjab Lahore Pakistan
***Correspondance:** sairabnaqvi5@gmail.com

Citation | Batool. S, Mahmood. S. A, Tahir. Z, Masood. A, Qureshi. J, Khan. B. Z. Hassan. S. M, "Assessment of Soil Erosion and Neotectonics Geomorphology of Bannu Basin using RS and GIS Techniques", IJIST, Special Issue.pp.387-407, June 2024
Received | June 09, 2024, **Revised |** June 13, 2024, **Accepted |** June 16, 2024, **Published |** June 24, 2024.

Soil erosion presents a significant environmental challenge in Bannu District, adversely impacting agricultural productivity and land sustainability. This research article offers a comprehensive approach to assessing and mitigating soil erosion risk in the region by utilizing the Revised Universal Soil Loss Equation (RUSLE) model in conjunction with hypsometric analysis. The study integrates various geospatial datasets, including mean annual rainfall, digital elevation models, soil maps, land use/land cover classifications, and satellite imagery. These datasets are essential for mapping the five key factors of the RUSLE model: Rainfall Erosivity (R), Soil Erodibility (K), Slope Length and Steepness (LS), Land Cover Management (C), and Support Practice (P). By mapping each factor individually and then integrating them, the study estimates soil erosion rates in Bannu District. Soil erosion risk is categorized into five levels, ranging from very low to excessive, to facilitate practical assessment. This classification assists in identifying areas that require immediate attention and intervention for sustainable land management and agricultural practices. The study highlights the benefits of combining Remote Sensing (RS) and Geographic Information System (GIS) technologies with the RUSLE model. This integration enables policymakers and land managers to evaluate and address soil erosion issues on a broader scale. Additionally, the study examines the role of hypsometry in understanding topography and erosion dynamics, incorporating topographic elements into the RUSLE model to explain soil erosion trends in Bannu District. Overall, this article provides a scientifically rigorous and practical soil erosion risk assessment for Bannu District. By leveraging the RUSLE model and GIS data with hypsometric analysis, the study offers valuable insights for addressing soil erosion and promoting sustainable land use in the region. The findings are intended to assist policymakers and stakeholders in safeguarding agricultural productivity and enhancing land sustainability in Bannu District.

Keywords: Soil Erosion; Geospatial Assessment; RUSLE; Hypsometric Integral; Drainage density; Transverse Topographic Asymmetry Factor.

Introduction:

Soil loss is recognized as one of the major global challenges of the 19th and 20th centuries, with significant impacts on agriculture, human health, and the global environment. Soils play a crucial role in supporting the production of valuable ecosystem services, yet anthropogenic activities and environmental factors continue to degrade soil quality [1]. Key drivers of soil degradation include population growth, land degradation, and desertification. Erosion, in particular, has numerous adverse effects that warrant serious concern [2][3]. It diminishes crop productivity and soil fertility by stripping away the fertile topsoil, reduces water storage capacity and quality, increases contamination and sedimentation in rivers and streams, and contributes to flooding by obstructing river flow with sediment layers. Additionally, soil erosion decreases the land's ability to absorb CO2, impacting greenhouse gas retention [5]. It is estimated that soil erosion affects approximately 10 million hectares of agricultural land annually, leading to decreased agricultural productivity, weakened economies, and increased food insecurity [7].

Globally, around 0.5-1% of sediment disrupts reservoir storage annually, and projections suggest that by the 2050s, many dams could lose half their current storage capacity, a troubling forecast [8]. In Asia, sediment occupies 40% of reservoir capacity, leading to substantial reductions in storage [9]. Developing countries, such as India and Iran, face severe soil degradation challenges, with India experiencing approximately 30 to 32.8 million hectares affected by water erosion [10], and Iran reporting an average annual soil degradation of 24 tons/ha/year [11]. In Pakistan, soil disturbance affects around 16 million hectares, with 11.2 million hectares (about 70%) suffering from water-induced erosion [12]. Worldwide, sediment production totals approximately 20 billion tonnes, with 80% of sediments reaching the oceans from major rivers [13].

Soil erosion poses severe threats to global food security and economic stability, particularly in regions with steep slopes and high rainfall. Annually, around 1 billion tonnes of fertile soil are lost and deposited in reservoirs or exported to the Arabian Sea. For instance, the Warsak Dam in Pakistan has lost 70% of its capacity due to sedimentation, highlighting the importance of estimating soil erosion to implement effective preventive measures [15]. Reducing soil erosion at such sites can enhance dam productivity and mitigate food security risks in agricultural areas.

The complexity of soil erosion arises from various influencing factors, including slope, precipitation, land use, altitude, and vegetation [16]. These factors, individually or combined, cause significant damage to agricultural lands and reduce reservoir capacities. Research has shown that land cover changes significantly impact soil loss, and climate change-induced increases in rainfall intensity exacerbate soil degradation [17]. Predicting soil erosion is crucial for mitigating these impacts. Effective soil erosion management relies on identifying risk areas and estimating erosion rates in tonnes per hectare per year. Various models have been employed globally to assess soil loss.

Risk mapping is a crucial step in addressing soil erosion challenges. Erosion models, such as the Revised Universal Soil Loss Equation (RUSLE), combined with GIS and remote sensing technologies, offer effective tools for evaluating and managing soil erosion. Traditional methods are often costly and time-consuming, making the RUSLE model an attractive alternative due to its simplicity, efficiency, and ease of implementation [20][21]. The integration of RUSLE with GIS and remote sensing data enhances accuracy and provides valuable insights for managing soil erosion [23][24].

Despite the RUSLE model's advantages, it has limitations, as it relies on available observations and may not always provide a complete picture of soil erosion outcomes [25][26]. However, it remains a practical approach due to the ease of data acquisition and its benefits for agriculture and waterway management. Previous research in regions such as Yunnan and

Pakistan's Potohar region has demonstrated the effectiveness of the RUSLE model in assessing soil degradation [27][28]. The RUSLE model, combined with GIS, provides a robust framework for estimating soil erosion and developing strategies to address soil disturbance [23][8][28].

The goal of this study is to create a soil loss profile for Bannu District to quantify soil erosion. The RUSLE model will be used alongside Remote Sensing and GIS to generate detailed maps. This approach aims to identify and mark areas of active deformation in the Bannu Depression. The main objective is to develop Iso Base and Transverse Topographic Asymmetry maps for the Bannu region to recognize neo-tectonic activity. The study will also analyze whether changes in drainage are tectonically induced or geologically controlled. By pinpointing erosion hotspots and contributing factors, the study will enable more targeted interventions, potentially improving agricultural output, preserving biodiversity, and extending dam lifespans.

Justification:

- The Bannu Depression is selected for study due to its location and tectonic activity.
- The availability of free remote sensing data facilitates research in this area.
- Iso Base and drainage basin asymmetry maps are being developed for the first time in this region.

Materials and Methods:

Study Site:

The research will be conducted in the Bannu Basin, located in the southern part of Khyber Pakhtunkhwa, Pakistan [32]. The coordinates are 32°43' to 33°06' North latitude and 70°22' to 70°57' East longitude. Bannu District is bordered by the Waziristan Mountains to the west, Kohat to the north, and small hill ranges to the south and east, with the Gomal Plain to the south and the Indus Plain to the east. Covering approximately 1,227 square kilometers, including 74,196 hectares of cultivated land, it is part of the Trans Indus District in the Northwest Frontier Province. The region is home to around 400 communities, primarily from the Bannuchi, Marwat, and Wazir tribes. Temperatures can reach up to 48°C in the hottest months and drop to around 6°C in the coldest months [33]. The rainy season lasts from January 9th to October 25th, with August being the wettest month, averaging 2.0 inches of precipitation. The region experiences a dry period from October 25th to January 9th.

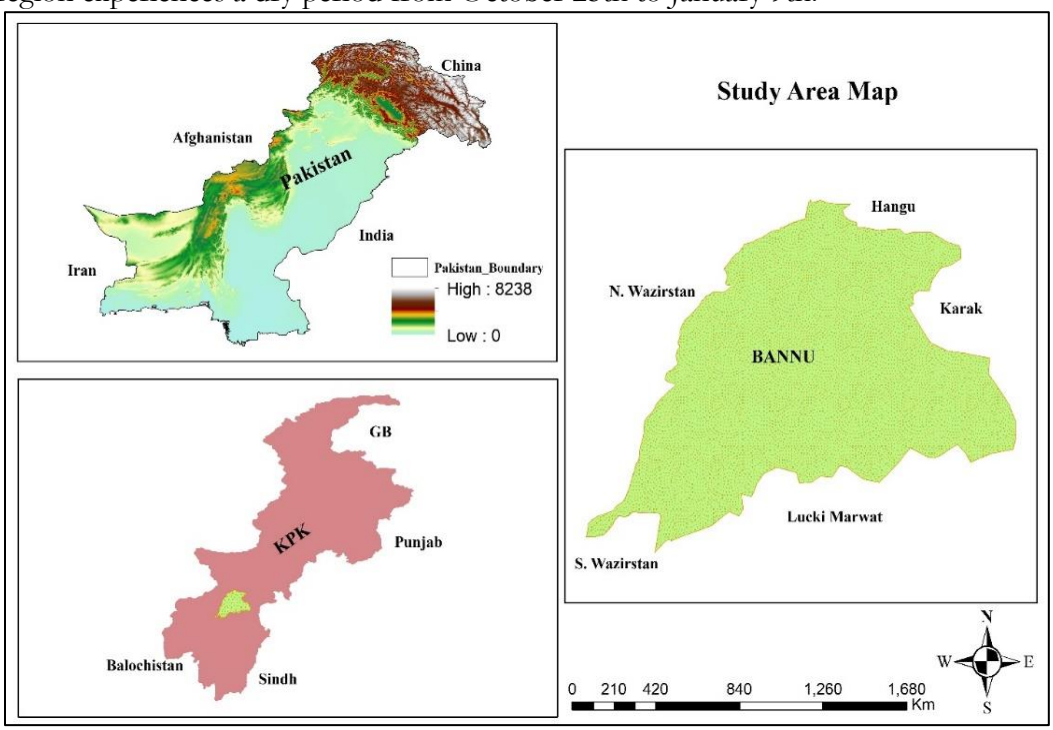

Figure 1: Location of study area.

Data Source Processing:

The Revised Universal Soil Loss Equation (RUSLE) has been effectively applied in various environments, including mountain ranges, tropical waterways, extensive watersheds, agrarian landscapes, and regions with distinct dry and wet seasons or continuous land use/cover changes. It has also been used to assess croplands and advancements. The RUSLE model relies on three main datasets for accurate soil erosion estimation:

- **Climate and Surveying Data:** This includes monthly rainfall and temperature values, essential for calculating the rainfall erosivity (R) and slope length and steepness (LS) factors.
- **Surface Cover Data:** Information from the land cover dataset, which provides details about vegetation and surface conditions, is used to determine the land cover management factor (C).
- **Soil Erodibility Data:** The soil erodibility factor (K) is calculated using soil survey and characterization data, which detail the soil's susceptibility to erosion.

These datasets are crucial for accurately assessing soil erosion and developing effective soil conservation measures.

Table 1: Description of data sources and its types

Type of data	Data sources	Description
Digital Elevation Model (DEM)	Earth Explorer (usgs.gov)	SRTM DEM (30 s resolution) Grid format
Soil data	Food and Agriculture Organization of the United Nations https://www.fao.org	FAO Digital soil Map of the World (DSMW)
Rainfall data	https://www.pmd.gov.pk/en/	Rainfall data yearly annual period
Satellite images	Earth Explorer (usgs.gov)	Landsat 8, 30m Resolution

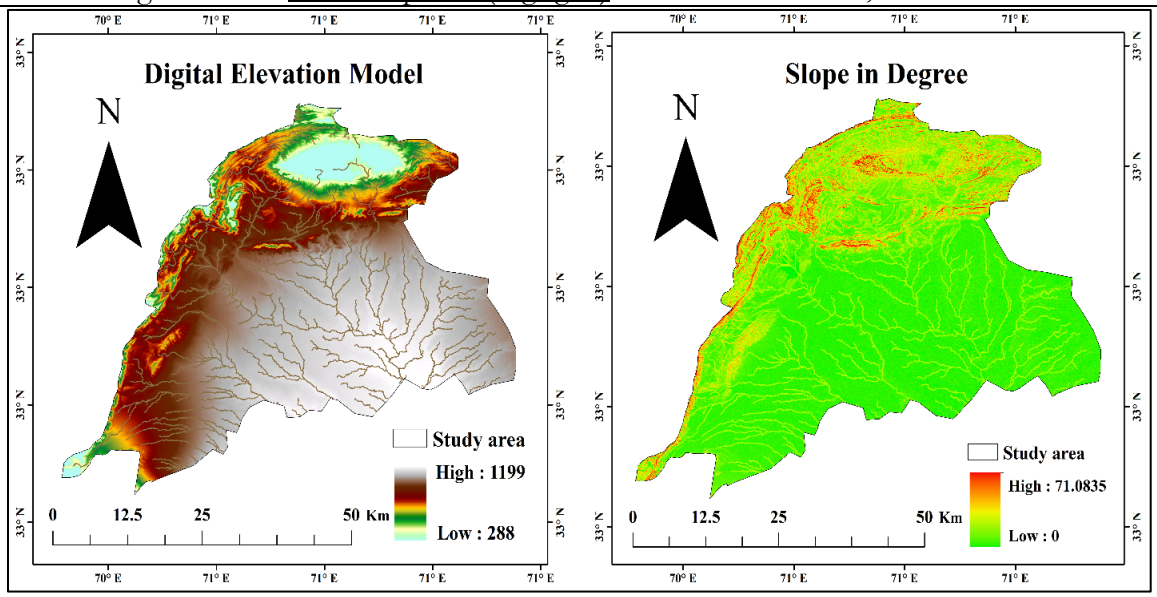

Figure 2: DEM and Slope of Bannu Basin.

RUSLE Model:

The RUSLE model is widely utilized for estimating soil erosion parameters. Researchers typically rely on a combination of meteorological data, soil and geological maps, remotely sensed satellite images, empirical equations, and digital elevation models (DEM) from diverse sources to predict these values. This article details the process of developing the model variables and presents the results. Annual average soil loss is calculated using the RUSLE model, which incorporates the five components outlined in Equation 1 [34].

$$A = R \times K \times LS \times C \times P \quad (1)$$

In the RUSLE model, "A" represents the mean annual soil loss in tons per hectare per year (t ha^{-1} $year^{-1}$), "R" denotes the rainfall erosivity factor measured in millimeters of water per hectare per year (MJ mm ha^{-1} h^{-1} $year^{-1}$), "K" is the soil erodibility index in metric tons per cubic meter per meter of water (t hr./MJ mm), "LS" is the topographic factor reflecting the length and steepness of slopes (dimensionless), "C" signifies cover management, akin to cropping management (also dimensionless), and "P" represents support measures or practice controls (dimensionless).

Erosion was calculated using the mathematical feature map, while all other components were derived independently from raster data. The area was delineated using the ArcGIS (10.8) mapping and analysis technique. To compute the RUSLE variables, a range of equations was applied, with satellite imagery and digital elevation model data serving as inputs. Table 1 provides details on the data sources, equations used, and the analysis process. The research involved an extensive review to identify the most accurate equations for computing the variables, selected for their ability to produce estimates consistent with published ground erosion observations. Further details on the derivation of each variable are discussed in the following sections; a visual representation of this process is illustrated in Figure 2.

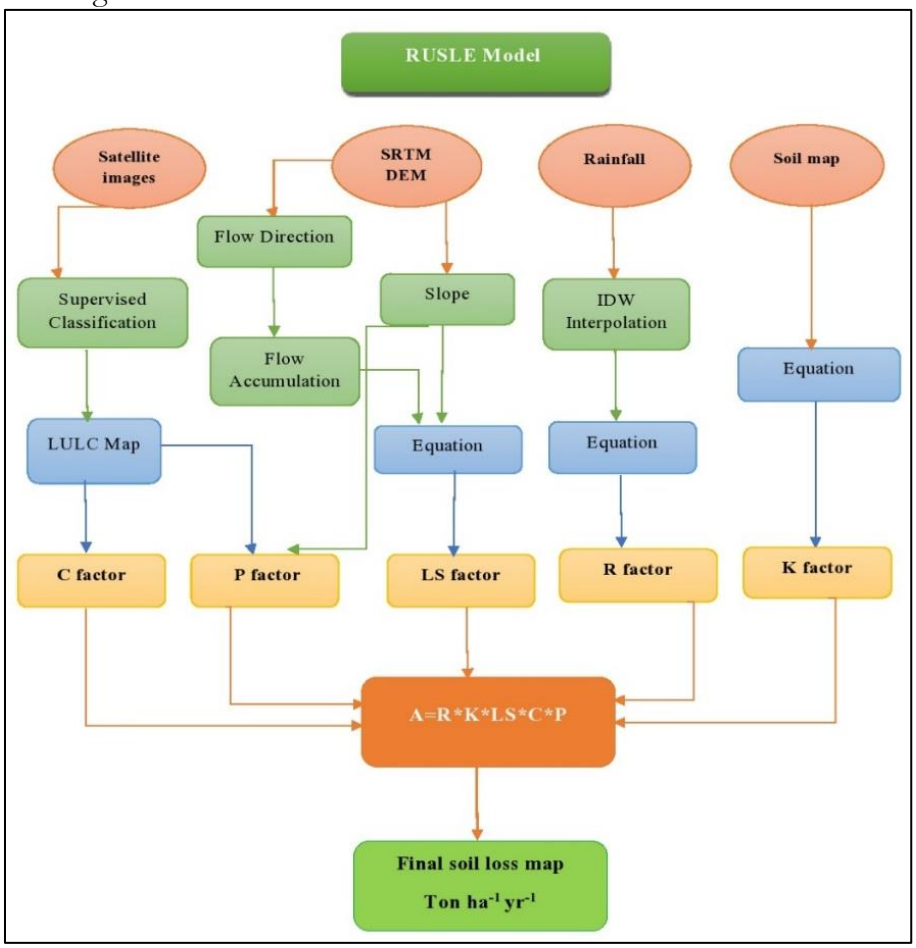

Figure 3: Flowchart of study area

R_Factor:

The component related to annual rainfall is vital for assessing the overall amount and intensity of precipitation. Monthly precipitation data spanning ten years (2012-2022) were gathered from the Pakistan Meteorological Department for each of the five weather stations in the study area. This data, expressed in millimeters, is crucial for calculating the rainfall erosivity

factor (R); higher annual precipitation corresponds to a higher R-value. By determining the average annual rainfall, the R factor can be calculated. To map rainfall distribution across the region, the inverse distance weighting (IDW) method was utilized in ArcMap. IDW is widely regarded as an effective tool for estimating precipitation patterns across a given area [35][36][37]. According to Numan [38], the following equation is considered the most accurate for calculating R.

$$R = -8.12 + 0.562 \times PCP \quad (2)$$

PCP indicates the average annual precipitation in mm.

Topographic LS Factor:

In this study, the L and S variables in the RUSLE model capture the impact of topography on erosion rates. Soil erosion and overland flow are generally higher with increased slope length and steepness [39]. We used the Digital Elevation Model (DEM) within the ArcGIS environment to calculate the LS (length and steepness) value, which provides detailed information about slope characteristics across the landscape. The LS calculation considered both flow accumulation and slope steepness. By integrating slope steepness and flow accumulation into the DEM using the ArcGIS Spatial Analyst add-on, we determined the runoff accumulation rate and slope. To derive the LS factor for our analysis, we applied Equation (3) as proposed by Moore and Burch [40][41].

$$LS = \frac{(\text{Flow accumulation} \times \text{CellSize})^{0.4}}{22.13} \times \frac{(\text{SinSlope})^{1.3}}{0.0896} \quad (3)$$

Where "Flow Accumulation" refers to the total upslope area contributing to each grid cell, and the "LS Factor" combines the length and steepness of slopes. The 'Cell Size' variable indicates the dimensions of a single grid cell, while 'Sin slope' represents the slope's angle in sine terms.

Soil Erodibility (SE) K_Factor:

The K_Factor measures the ease with which soil particles can be detached and transported by precipitation and runoff. It is primarily influenced by soil texture, organic matter content, structure, and permeability. The SE, or "rate of erosion per unit of the erosion index from a typical unit plot of 22.13 meters in length with a slope gradient of 9%" [42], reflects the rate of soil loss relative to the rainfall erosivity (R) index.

Cover Management Factor (C):

The C factor characterizes soil loss in relation to land use/land cover (LULC) classifications. Calculating the C factor requires information about soil management practices, crop type, soil moisture, and surface variations [43]. In this study, we determined the C factor using LULC categorization, following the methodologies outlined by [44][45]. We derived the C parameter from the LULC map of the basin. Table 2 lists the values for the cover management factor, which range from 0 to 1. The C-factor is crucial for soil erosion modeling, as it estimates an area's susceptibility to soil loss. Higher C-factor values indicate greater vulnerability to erosion, suggesting less effective vegetation cover or management practices in those areas.

Table 2: C factor for LULC Classes

Sr. No	Land Cover	C_Factor
1	Grass Land	0.7
2	Forest Cover	0.004
3	Water Bodies	0
4	Crop Land	0.65
5	Buildup Area	0
6	Snow Cover	0
7	Bare Land	1

Erosion Control Practice (P) Factor:

The P-factor in soil erosion modeling represents the effectiveness of erosion control practices in mitigating soil loss under specific topographic conditions, particularly concerning up-and-downhill plowing. This factor accounts for various land treatments and measures designed to prevent soil particle movement and minimize erosion. Erosion control practices such as contouring, compaction, constructing sediment basins, and implementing erosion control structures influence the P-factor. In Pakistan, limited efforts have been made to implement such erosion control practices, resulting in a general lack of comprehensive erosion control measures across the region. Consequently, for the entire study area, the P-factor was assigned a value of 1, reflecting the absence of specific erosion control practices and minimal resistance to soil erosion [10][46].

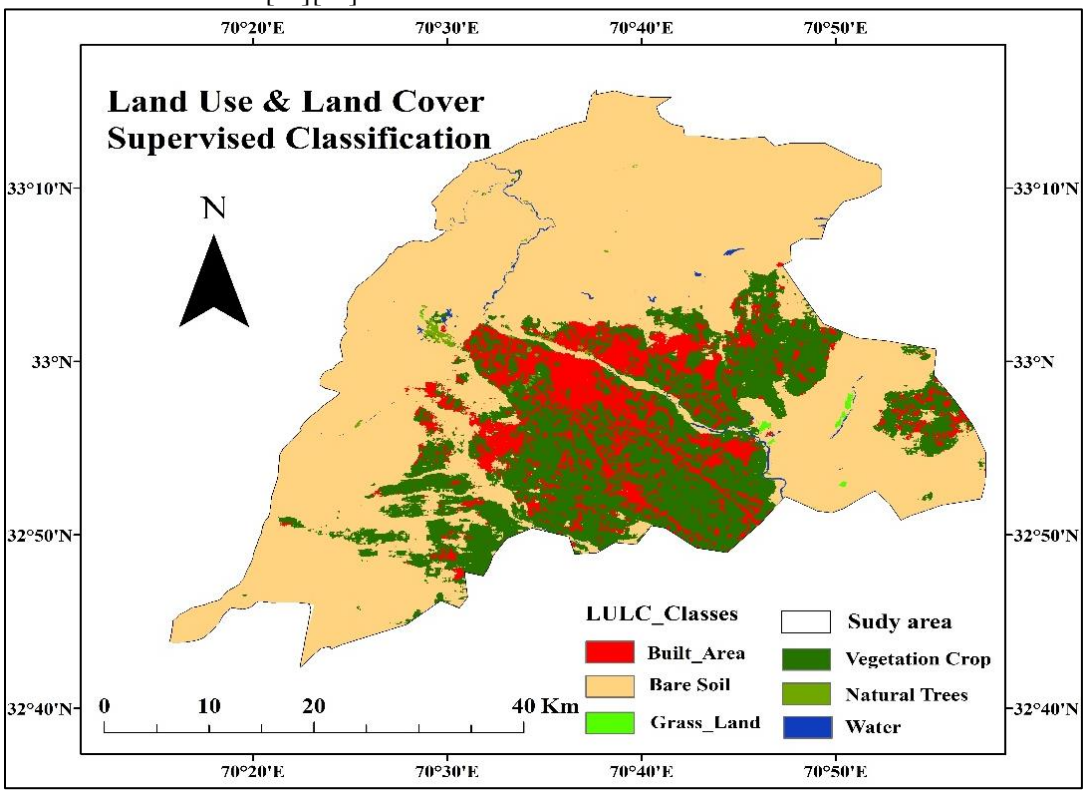

Figure 4: Land Use Land Cover Classification of Bannu

Table 3 : List of software used for this research

Software Name	Application
Arc GIS 10®	For Map making and Re-projection
ENVI	Import and Export
MATLAB 7.6.0 (R2008a) Robocop version	Extraction geomorphic Indices and DEM Processing

Hypsometric Integral:

The hypsometric integral of Bannu Basin is a geomorphological metric used to analyze the elevation distribution within the basin. This integral is computed by graphing the cumulative area of the basin against its cumulative elevation and calculating the area under the resulting hypsometric curve. The hypsometric integral provides valuable insights into the basin's overall shape and relief characteristics, enabling geologists and geomorphologists to understand its geological evolution, tectonic activity, and erosional history. By examining the hypsometric integral of Bannu Basin, researchers can gain a clearer understanding of the basin's geomorphic development and infer landscape processes, uplift rates, and tectonic influences that have shaped the region over geological timescales.

Transverse Topographic Basin Symmetry:

Transverse topographic basin symmetry is an innovative technique used to assess the asymmetry of topographic basins and differentiate between random and regional stream migration patterns. While this method does not provide definitive evidence of ground tilting or tectonic movement, it can help identify factors related to ground tilting in neotectonic regions, particularly where active faults are concealed or poorly exposed. Stream migration can be influenced by both external forces, such as monoclinal shifting and tectonic tilting, and internal fluvial processes. External forces consistently affect the lateral migration of streams, depending on factors like stream orientation, size, and substrate resistance. Internal fluvial processes, however, influence stream migration independently, leading to a lack of a well-defined mean migration direction for a stream population.

Drainage-basin symmetry methods compute the mean migration direction for all streams of a certain order or higher, allowing differentiation between migration due to external forces and internal processes. By examining the deflection of the active meander belt from the drainage basin midline, an asymmetry vector is determined for each valley segment of a specific length. This data is then used to calculate a mean vector and statistically assess whether it is likely the result of non-random processes. This technique is particularly useful for evaluating recent tectonic activity in regions with poorly exposed or absent surface faults. Basin asymmetry, while indirect, relies on geomorphic variations, stream organization, and watershed asymmetry to assess tectonic impacts. Large water channels, being sensitive to tectonic activity, can indicate subsidence or uplift through changes in tributary directions.

ISO Base Level:

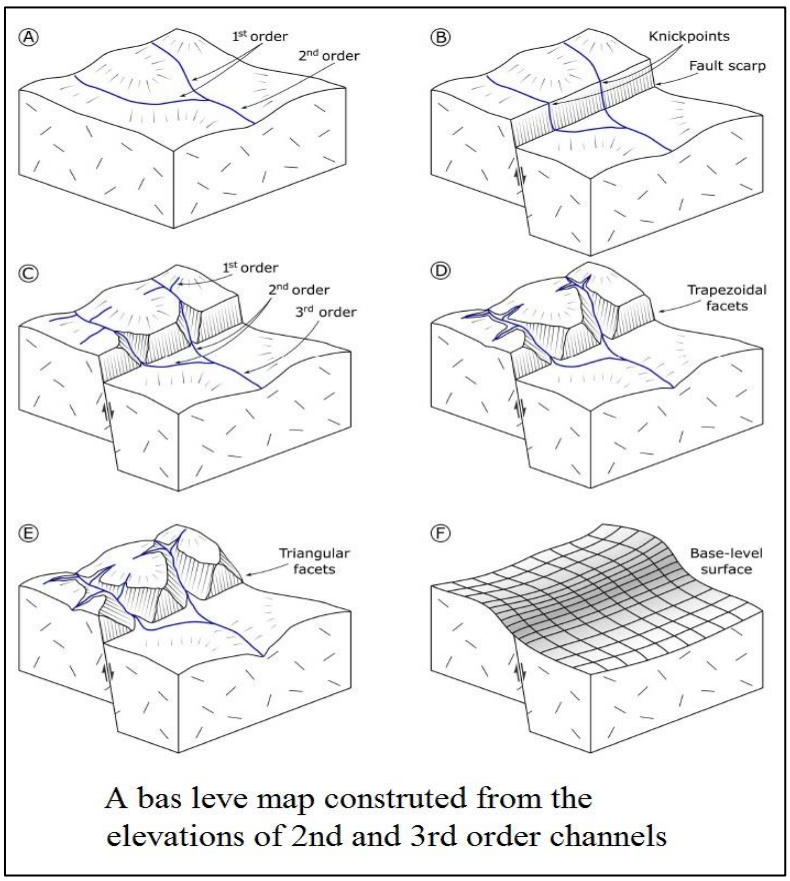

Figure 5: Generation of base level map

Base-level maps, or "isobase maps" as originally defined by Filosofov (1960), illustrate the relationship between geology and valley order. These maps can be seen as an "enhanced" form of the initial topographic surface, from which the "noise" of low-order stream

disintegration has been removed. This approach allows for the identification of areas with potential tectonic impact, even within lithologically uniform regions. The concept of base level was defined as a level "below which dry grounds cannot be eroded." While sea level is the ultimate base level, some researchers have suggested that local base levels can be defined according to different geological or temporal conditions across areas or even within the same watershed.

Base-level maps reflect the relationship between valley order and geology. Valley order refers to the relative position of tributary segments in a stream network, where streams of similar orders correspond to similar geomorphological events and have comparable topographical ages. Each base-level surface is associated with specific erosional stages and can be seen as a result of erosional-tectonic events, predominantly the most recent ones. Stream networks serve as an authentic indicator of tectonic activity. Stream long profiles are sensitive to various forces, including climate and lithology, with lithological boundaries between rocks of differing erosional properties affecting channel slope and local base level, even without significant tectonic deformation.

Results and Discussion:

Topographic LS Factor:

Figure 6 illustrates the variation in the length-slope (LS) factor across the Bannu Basin. The LS factor, which combines slope length and steepness, significantly influences soil erosion potential. The map displays LS values throughout the basin, highlighting areas with varying erosion susceptibility. Regions with higher LS values, indicating steeper and longer slopes, are more prone to erosion. Conversely, areas with lower LS values, characterized by gentler and shorter slopes, are less likely to experience significant erosion. The LS factor values range from 0 to 8.75 within the study area, with higher values correlating to increased erosion risk and lower values indicating reduced erosion potential. This variation in LS factor is crucial for assessing erosion control needs and implementing preservation strategies in the Bannu Basin.

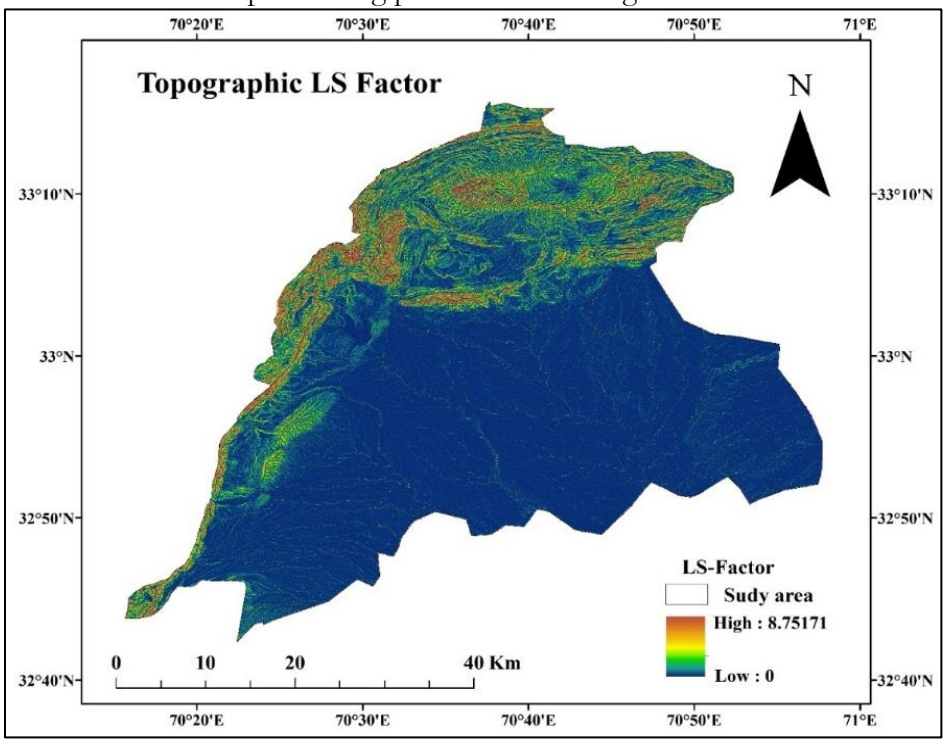

Figure 6: Length and Slope (LS) factor

Rainfall Erosivity Factor:

The R-factor map for the Bannu Basin was developed using mean annual rainfall data collected from weather stations. To generate a detailed depiction of rainfall erosivity across the

study area, the Inverse Distance Weighting (IDW) method was used for interpolation. Figure 7 displays the spatial distribution of R-factor values across the Bannu district, ranging from 26.9 to 29.8 MJ mm/ha/h/year. The R-factor, a crucial element of the Revised Universal Soil Loss Equation (RUSLE) model, measures the erosive potential of rainfall in terms of its capacity to induce soil erosion. There is notable variability in R-factor values across the region. Areas with R-factors approaching 29.8 MJ mm/ha/h/year experience more intense and erosive rainfall patterns, leading to increased susceptibility to soil erosion due to the higher impact energy of raindrops and surface runoff. In contrast, regions with lower R-factor values, around 26.9 MJ mm/ha/h/year, encounter less intense and erosive rainfall, resulting in a reduced likelihood of soil erosion. This reduced erosion potential can be attributed to factors such as milder rainfall intensity and a higher capacity for water infiltration into the soil.

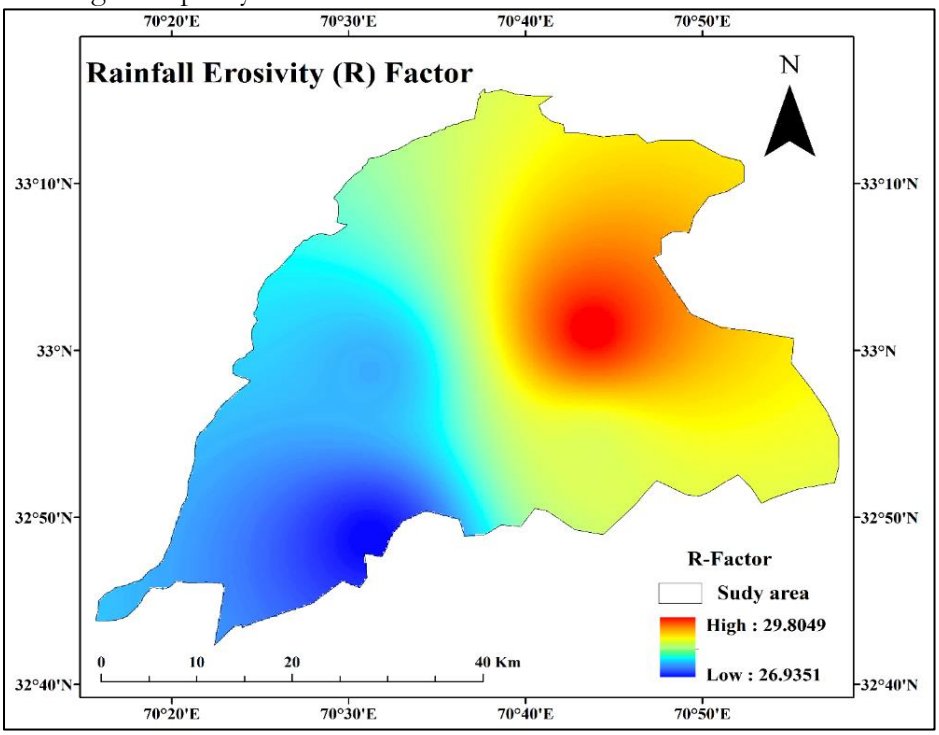

Figure 7: Rainfall Erosivity (R) factor

Soil Erodibility Factor:

Figure 9 illustrates the distribution of K values across the Bannu region, which range from 0.19 to 0.27, indicating low-to-moderate soil erodibility in the area. The K factor quantifies the susceptibility of soil to erosion, with lower K values reflecting soils that are less prone to erosion and higher values indicating greater erosion potential. To further elucidate the spatial variation in soil erodibility, the K factor is categorized into two main types: lithosols and haplic xerosols. The map employs a color scheme to represent these categories, with green denoting areas of low erosion capacity and blue indicating regions with high erosion capacity. The gradient from green to blue signifies increasing soil erosion potential across the Bannu region. Lithosols generally exhibit low soil erodibility, indicating a higher resistance to erosion, whereas haplic xerosols are more prone to erosion under erosive conditions.

Cover Management Factor:

Figure 4 shows the land cover classification in the Bannu region, divided into six categories: bare land, built-up areas, water bodies, natural trees, vegetation crops, and grassland. Figure 9 depicts the "C factor" of the Revised Universal Soil Loss Equation (RUSLE) model. The "C factor," representing the "cover and management" aspect of the RUSLE model, measures the impact of land cover and management practices on soil erosion. This factor varies according to the type of land cover and management practices in the region. Natural forests and

grasslands typically have high C factors due to their vegetation cover, which provides substantial protection against erosion. Detailed information on classification accuracy is available in Table 2.

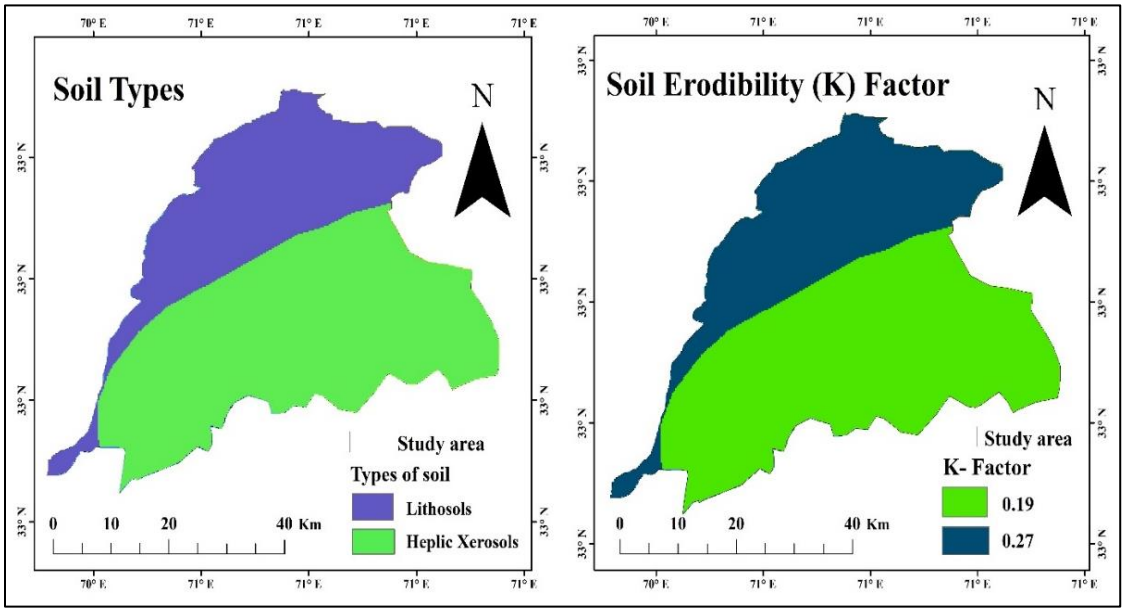

Figure 8: Soil Types and Soil Erodibility factor

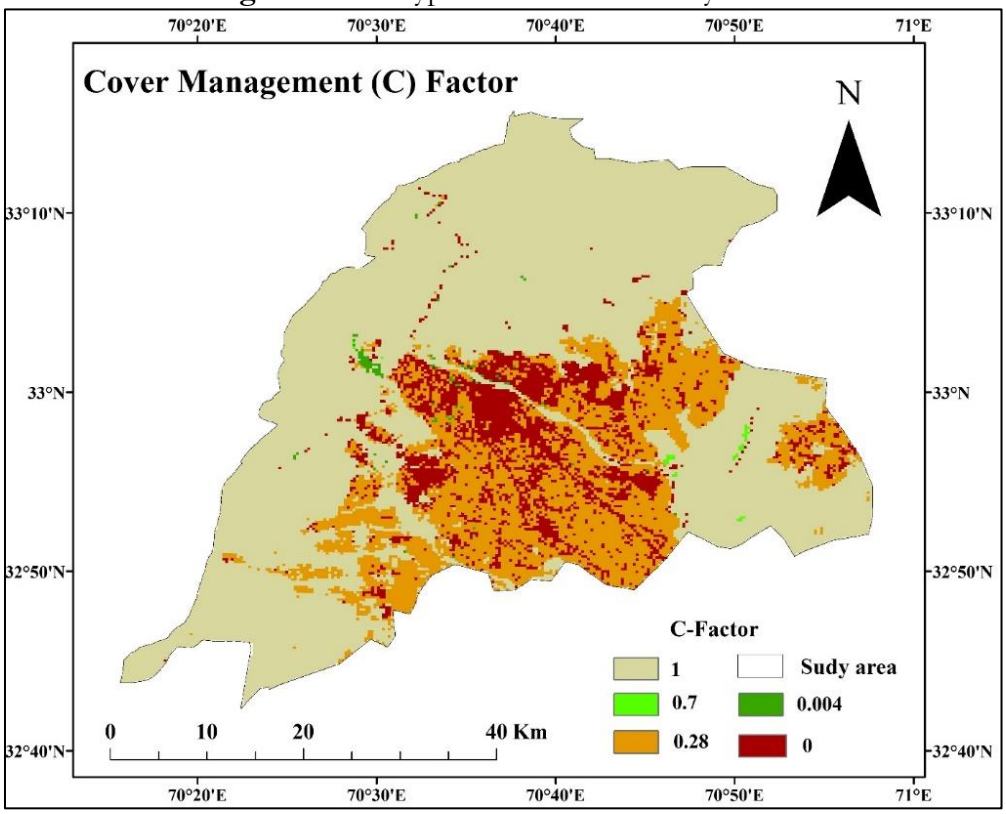

Figure 9: Cover Management C factor of Bannu basin

Soil loss Estimation:

Spatial variations in soil erosion patterns within the study region were identified, necessitating the categorization of areas based on their erosion risk for more straightforward analysis. Accurate assessment of soil erosion hazards is crucial for pinpointing high-risk areas and devising effective preventive measures. To evaluate soil erosion risk, this research employed a classification system based on boundaries established by the OECD, a framework commonly

used in regional studies. This classification approach aligns with methods applied in prior research conducted in the same general area.

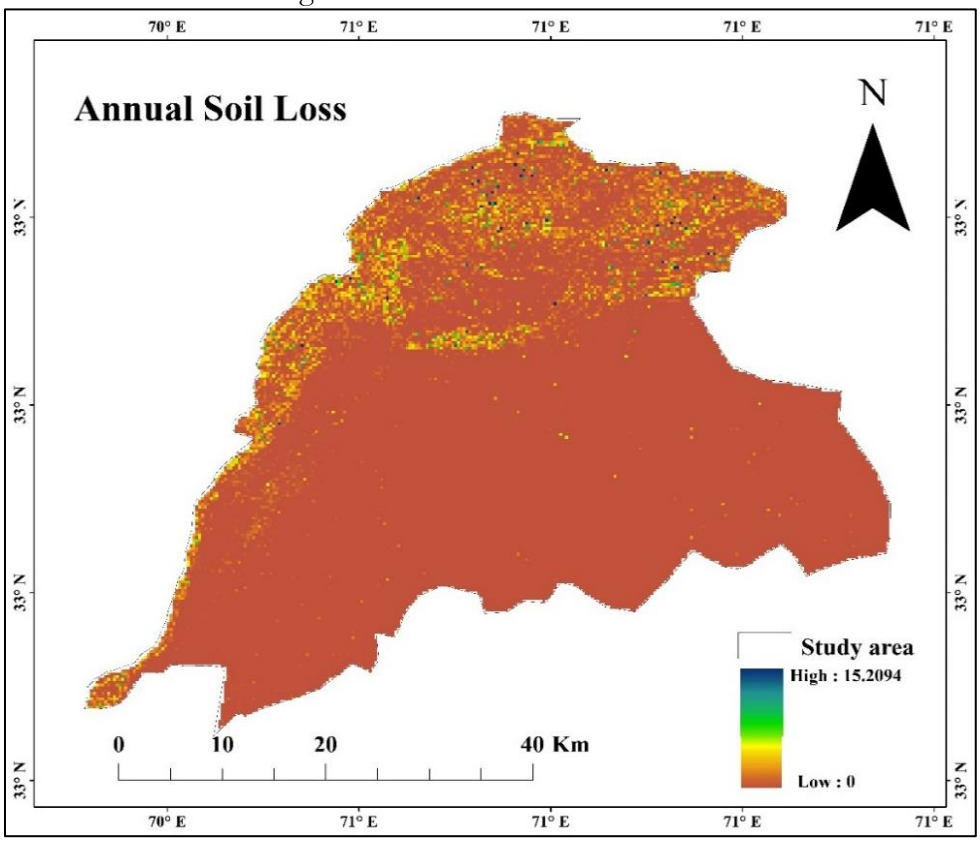

Figure 10: Annual Soil loss map for study area

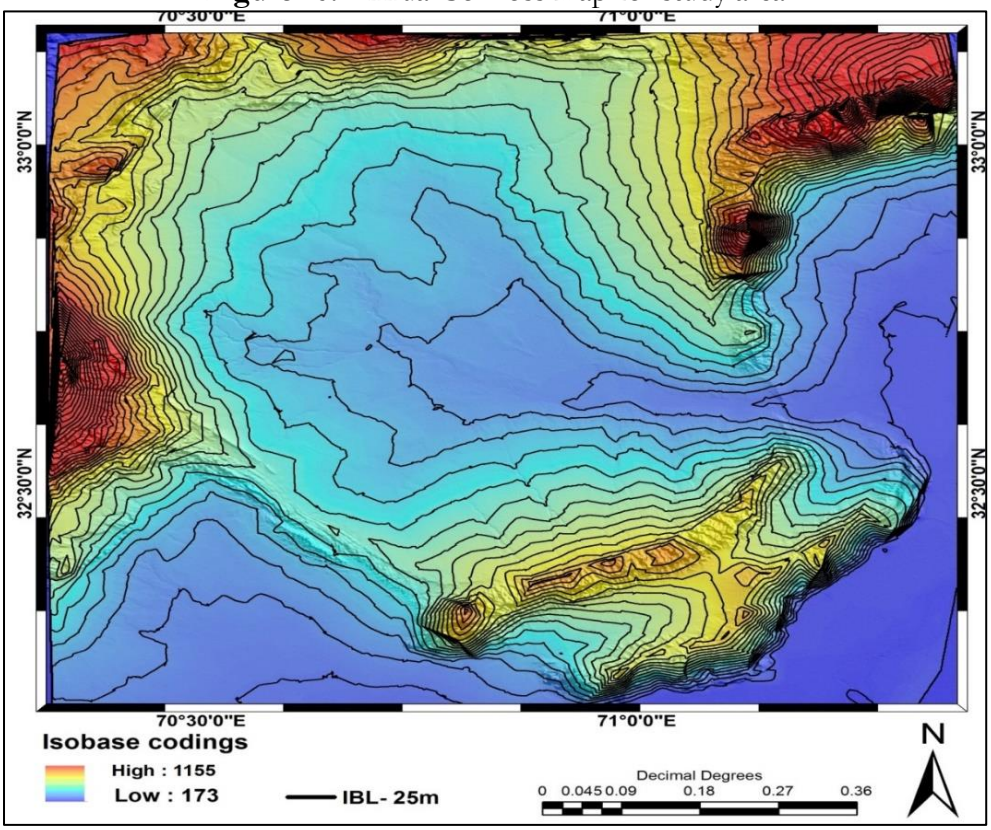

Figure 11: Iso Base map of Bannu with Contours of 25m

These erosion maps were created by consolidating the relevant parameters and applying Equation (1) using the raster calculator in ArcGIS. The resulting maps were then calibrated and analyzed to assess the severity of soil erosion risk within the watershed. In these maps, higher parameter values indicate greater erosion rates, while lower values represent reduced sediment yield. Figure 10 visually depicts the annual soil loss, ranging from 0 to 15 tons per hectare. The map illustrates spatial variations in soil erosion, with some areas showing low soil loss while others exhibit higher levels. The findings indicate that bare areas and highlands with steep slopes are particularly vulnerable to soil erosion, as highlighted by the map.

ISO Base Level:

Iso Base maps facilitate the examination of landscape variations and changes in stream Strahler orders. These maps display lines of equal uplift, indicating different erosional stages. For the Bannu depression, Iso Base maps have been generated for the first time, with contours created at 25m, 50m, 75m, and 100m intervals using ArcGIS 10. The resulting maps provide valuable insights into tectonic activity: thicker Iso Base lines in red highlight areas of significant tectonic activity, while broader contour lines represent regions with relatively lower tectonic activity. The Iso Base contour lines also clearly depict various stages of erosion, offering a comprehensive understanding of the region's geomorphic development and providing important information for analyzing tectonic influences and landscape processes.

Areas of high tectonic activity are depicted on the map with thicker Iso Base lines in red, while regions of relatively lower activity are shown with wider contour lines. Due to the 50m contour interval used in the map, the contours are broader compared to those on a map with a 25m interval. However, within the same regions of high tectonic activity, the contour lines appear thicker.

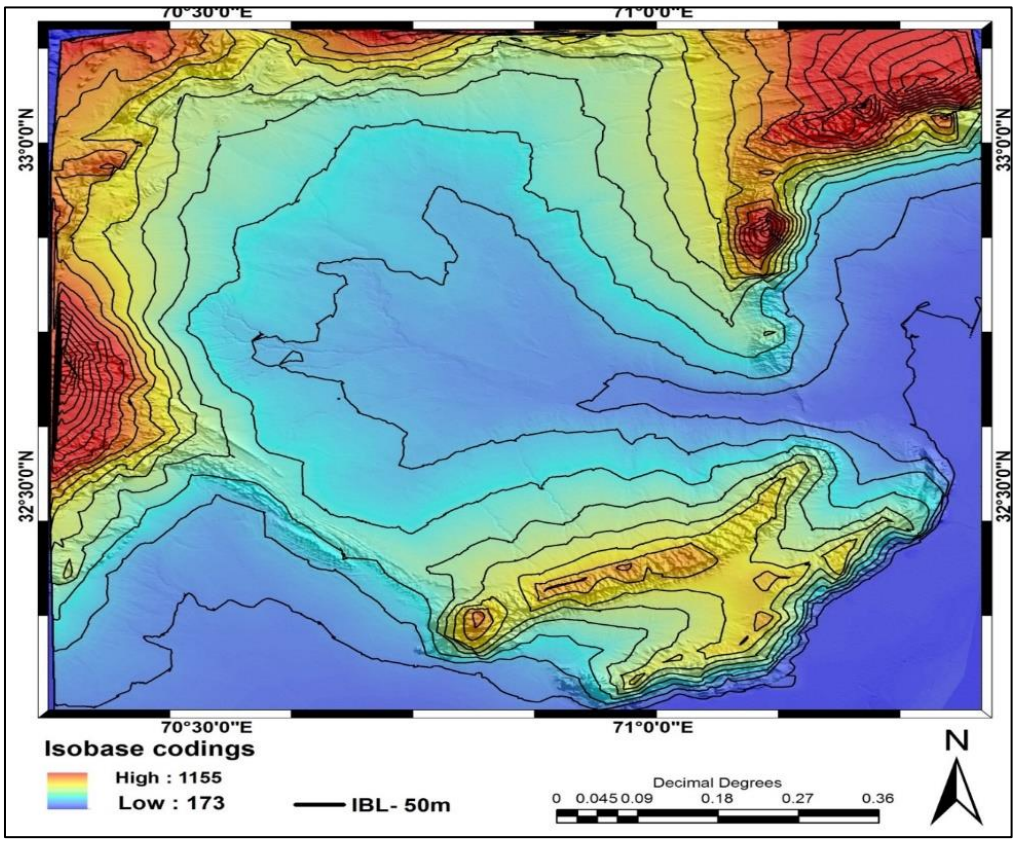

Figure 12: Iso Base map of Bannu with Contours of 50m

In this map, contours are generated at a 75m interval, resulting in broader lines compared to those at 25m and 50m intervals. However, the contour lines remain thicker at the same locations.

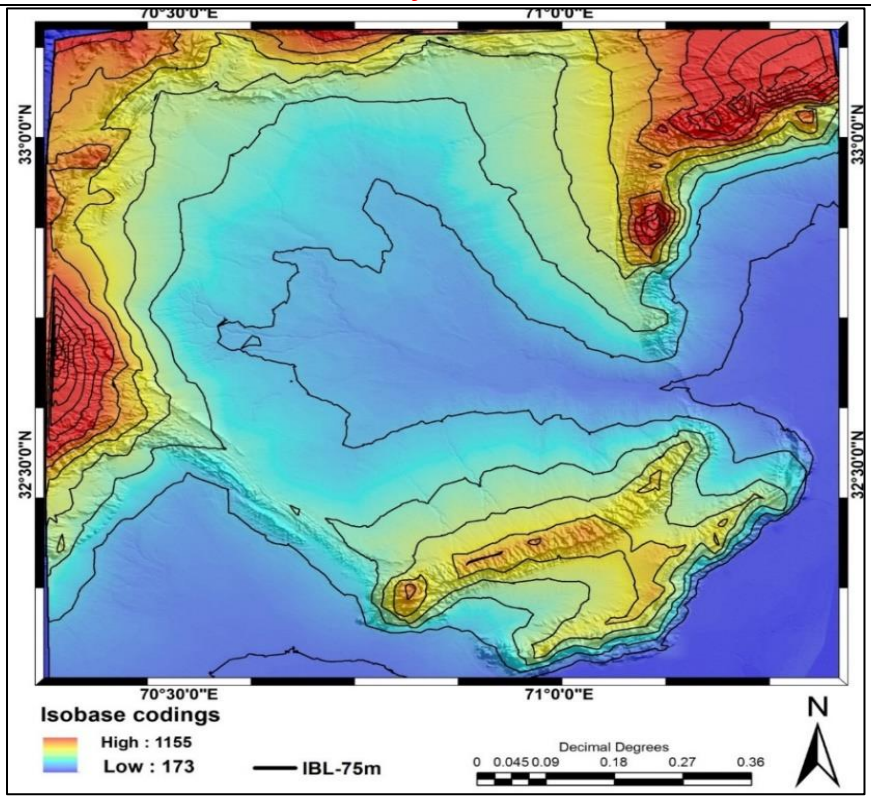

Figure 13: Iso Base map of Bannu with Contours of 75m

In this map, contours are generated at a 100m interval, making them broader compared to those at 25m, 50m, and 75m intervals. However, the contour lines are still thicker at the same locations as seen in the previous maps.

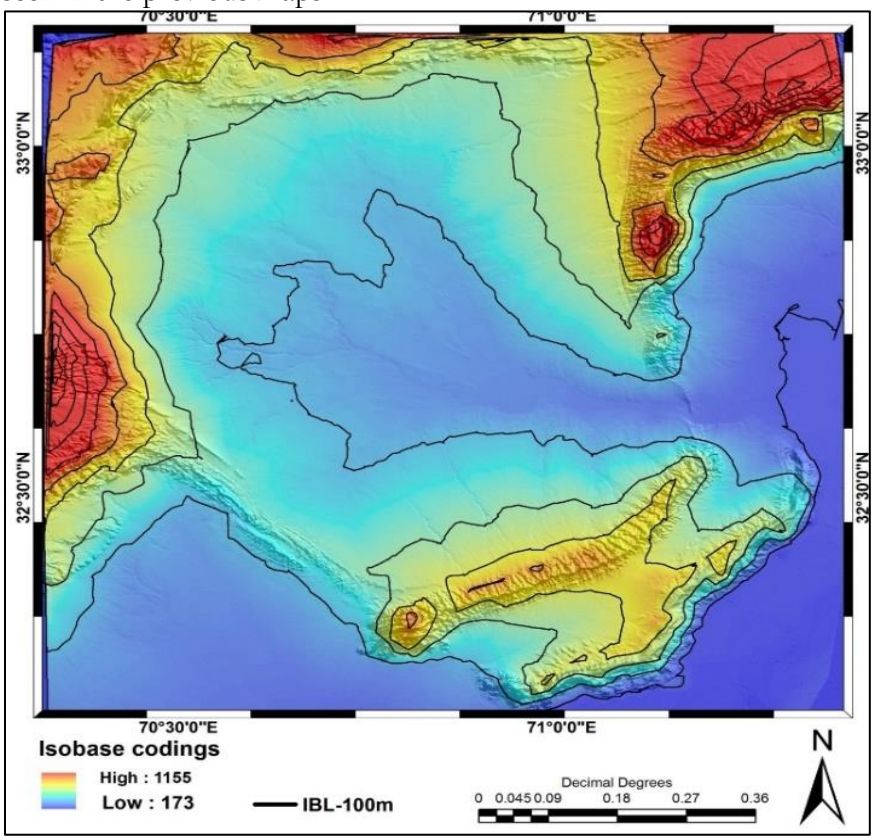

Figure 14: Iso Base map of Bannu with Contours of 100m

Aspect Map:

An aspect map of Bannu illustrates the directional orientation of the region's slopes. This map is essential for understanding the direction each point on the landscape faces. Aspect is measured in degrees, where 0° denotes a north-facing slope, 90° an east-facing slope, 180° a south-facing slope, and 270° a west-facing slope.

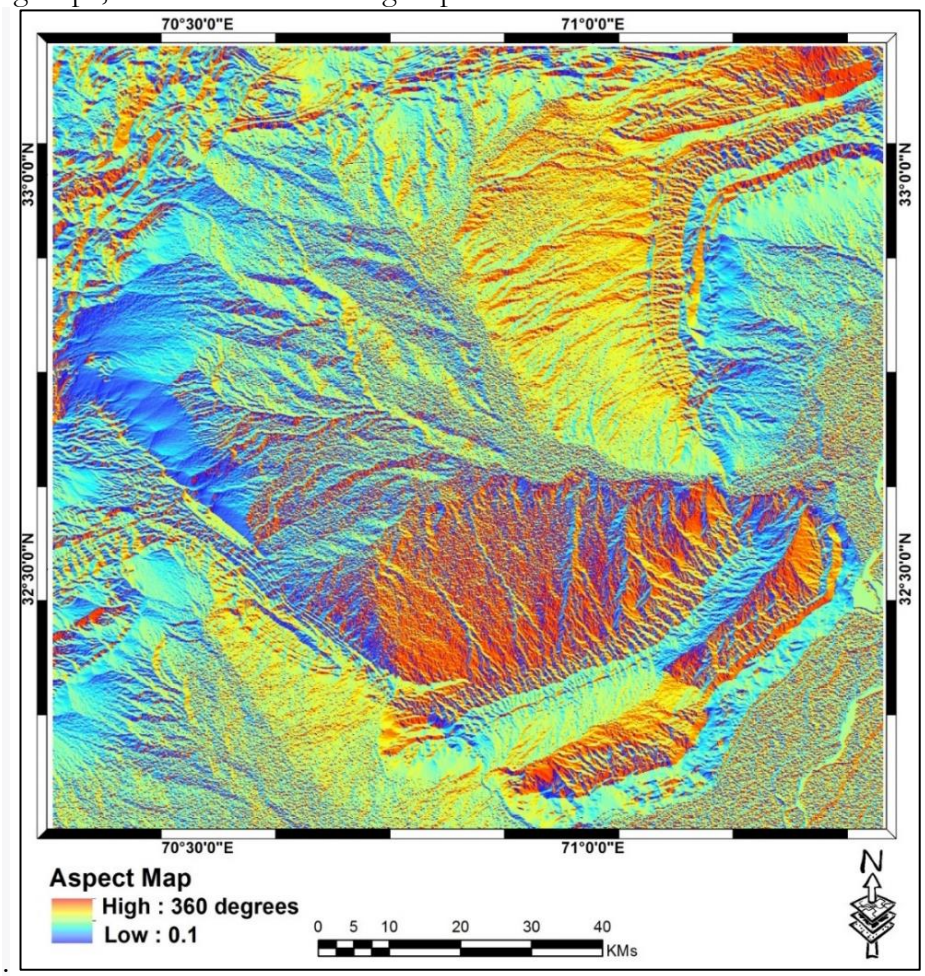

Figure 15: Aspect map of Bannu Depression.

Shaded Relief Map:

The shaded relief map of Bannu highlights the region's topography and terrain features through the use of light and shadow effects. By simulating illumination from a specific light source, this map creates a three-dimensional appearance of the land surface. Elevations and landforms are represented by varying shades of gray or color, with higher elevations appearing lighter and lower elevations appearing darker.

Transverse Topographic Basin Asymmetry:

This method is a valuable tool for assessing neo-tectonic activity by examining shifts in the drainage basin midline. Drainage systems are highly sensitive to tectonic activity, as even minor elevation changes can significantly alter their configuration. The T-index, calculated using the formula \(T = \frac{Da}{Dd} \), measures the distances from the basin midline to the basin margin. To create a T-index map of the Bannu Depression, data from the 5th, 6th, and 7th Strahler stream orders were analyzed using the SRTM DEM in MATLAB. The resulting map displays arrows indicating the direction of river midline migration. Observations reveal that streams are migrating in a downward tilt direction due to uplift, suggesting active tectonic processes in the area. This map provides valuable insights into the region's geomorphic dynamics and aids in understanding neo-tectonic activity in the Bannu Depression.

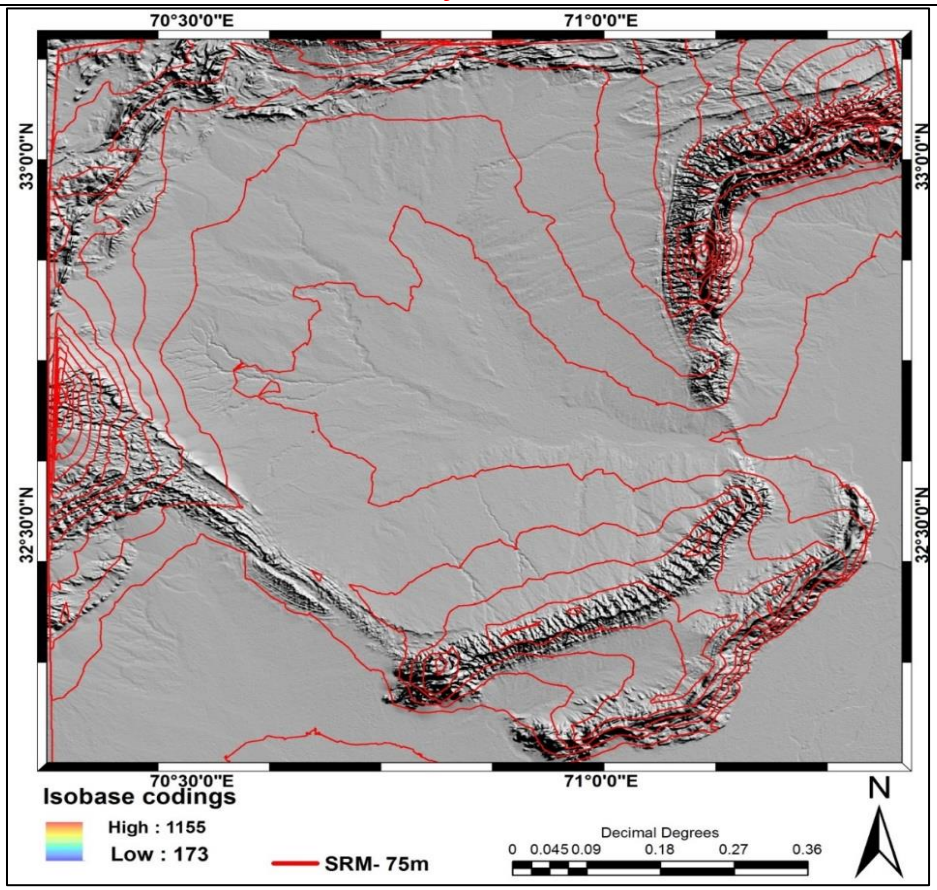

Figure 6: SRM of Bannu Depression

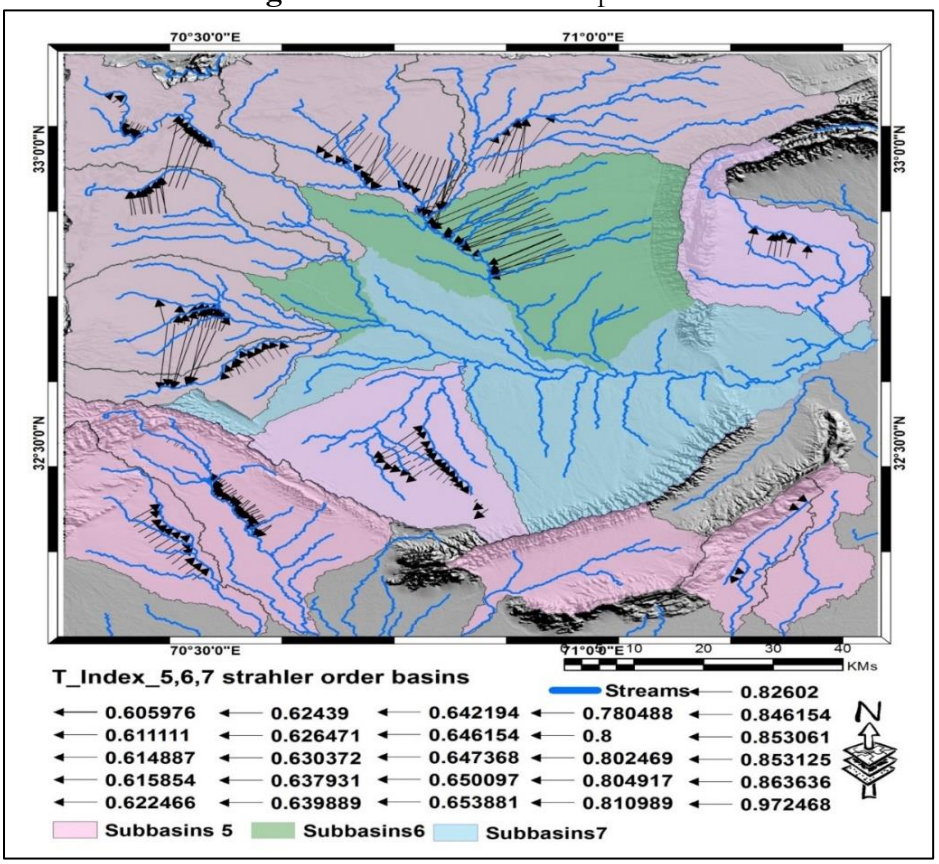

Figure 17: T-Index map of bannu basin

Conclusion:

In conclusion, the Revised Universal Soil Loss Equation (RUSLE) model has demonstrated its value as a cost-effective tool for estimating soil erosion rates across diverse regions. Its capacity to incorporate multiple factors—including rainfall intensity, soil erodibility, slope, land cover, and land management practices—enables a thorough assessment of soil erosion risk. By integrating RUSLE parameters with GIS software like ArcGIS, researchers and land managers can produce detailed soil erosion risk maps, which are essential for developing effective soil conservation and land management strategies. Hypsometry, the study of elevation distribution within a geographic area, is crucial for understanding the topographical features of a landscape. Hypsometric data and maps offer valuable insights into elevation ranges, highlighting low-lying and highland regions. ISO base maps, adhering to International Organization for Standardization (ISO) standards, provide reliable geospatial data, including administrative boundaries, transportation networks, hydrography, and elevation contours. In summary, combining the RUSLE model, hypsometry, and ISO base maps presents a powerful methodology for analyzing and managing soil erosion risks. These tools collectively enable a comprehensive evaluation of soil loss potential, landscape characteristics, and geographic context, which is vital for devising targeted soil conservation strategies and sustainable land management practices. As concerns about soil degradation and environmental resilience grow, the application of these tools is increasingly essential for protecting our natural resources and ensuring long-term ecological stability.

References

[1] D. A. Robinson et al., "Soil natural capital in Europe; A framework for state and change assessment," Sci. Rep., vol. 7, no. 1, pp. 1–14, 2017, doi: 10.1038/s41598-017-06819-3.

[2] S. D. Keesstra et al., "The significance of soils and soil science towards realization of the United Nations sustainable development goals," Soil, vol. 2, no. 2, pp. 111–128, 2016, doi: 10.5194/soil-2-111-2016.

[3] A. Gayen and S. Saha, "Application of weights-of-evidence (WoE) and evidential belief function (EBF) models for the delineation of soil erosion vulnerable zones: a study on Pathro river basin, Jharkhand, India," Model. Earth Syst. Environ., vol. 3, no. 3, pp. 1123–1139, 2017, doi: 10.1007/s40808-017-0362-4.

[4] A. El Jazouli, A. Barakat, A. Ghafiri, S. El Moutaki, A. Ettaqy, and R. Khellouk, "Soil erosion modeled with USLE, GIS, and remote sensing: a case study of Ikkour watershed in Middle Atlas (Morocco)," Geosci. Lett., vol. 4, no. 1, 2017, doi: 10.1186/s40562-017-0091-6.

[5] P. Borrelli et al., "An assessment of the global impact of 21st century land use change on soil erosion," Nat. Commun., vol. 8, no. 1, 2017, doi: 10.1038/s41467-017-02142-7.

[6] A. Gayen, S. Saha, and H. R. Pourghasemi, "Soil erosion assessment using RUSLE model and its validation by FR probability model," Geocarto Int., vol. 35, no. 15, pp. 1750–1768, 2020, doi: 10.1080/10106049.2019.1581272.

[7] H. Allafta and C. Opp, "Soil Erosion Assessment Using the RUSLE Model, Remote

Sensing, and GIS in the Shatt Al-Arab Basin (Iraq-Iran)," Appl. Sci., vol. 12, no. 15, 2022, doi: 10.3390/app12157776.

[8] P. Chuenchum, M. Xu, and W. Tang, "Estimation of soil erosion and sediment yield in the lancang-mekong river using the modified revised universal soil loss equation and GIS techniques," Water (Switzerland), vol. 12, no. 1, 2020, doi: 10.3390/w12010135.

[9] D. E. Walling, "Human impact on the sediment loads of Asian rivers," IAHS-AISH Publ., vol. 349, no. September 2009, pp. 37–51, 2011.

[10] A. Maqsoom et al., "Geospatial Assessment of Soil Erosion Intensity and Sediment Yield Using the Revised Universal Soil Loss Equation (RUSLE) Model," ISPRS Int. J. Geo-Information 2020, Vol. 9, Page 356, vol. 9, no. 6, p. 356, May 2020, doi: 10.3390/IJGI9060356.

[11] T. Khatoon and A. Javed, "Morphometric Behavior of Shahzad Watershed, Lalitpur District, Uttar Pradesh, India: A Geospatial Approach," J. Geogr. Inf. Syst., vol. 14, no. 03, pp. 193–220, 2022, doi: 10.4236/jgis.2022.143011.

[12] A. Ashraf, M. K. Abuzar, B. Ahmad, M. M. Ahmad, and Q. Hussain, "Modeling risk of soil erosion in high and medium rainfall zones of pothwar region, Pakistan," Proc. Pakistan Acad. Sci. Part B, vol. 54, no. 2, pp. 67–77, 2017.

[13] P. Thapa, "Spatial Estimation of Soil Erosion Using RUSLE Modeling: A case study of Dolakha District, Nepal," Jul. 2020, doi: 10.21203/RS.3.RS-25478/V4.

[14] H. Atoma, K. V Suryabhagavan, and M. Balakrishnan, "Soil erosion assessment using RUSLE model and GIS in Huluka watershed, Central Ethiopia," Sustain. Water Resour. Manag., vol. 6, no. 1, p. 12, 2020, doi: 10.1007/s40899-020-00365-z.

[15] A. R. Vaezi, M. Abbasi, S. Keesstra, and A. Cerdà, "Assessment of soil particle erodibility and sediment trapping using check dams in small semi-arid catchments," CATENA, vol. 157, pp. 227–240, 2017, doi: https://doi.org/10.1016/j.catena.2017.05.021.

[16] X. Wang et al., "Assessment of soil erosion change and its relationships with land use/cover change in China from the end of the 1980s to 2010," CATENA, vol. 137, pp. 256–268, 2016, doi: https://doi.org/10.1016/j.catena.2015.10.004.

[17] M. Zare, T. Panagopoulos, and L. Loures, "Simulating the impacts of future land use change on soil erosion in the Kasilian watershed, Iran," Land use policy, vol. 67, pp. 558–572, 2017, doi: https://doi.org/10.1016/j.landusepol.2017.06.028.

[18] S. Altaf, G. Meraj, and S. A. Romshoo, "Morphometry and land cover based multi-criteria analysis for assessing the soil erosion susceptibility of the western Himalayan

watershed," Environ. Monit. Assess., vol. 186, no. 12, pp. 8391–8412, 2014, doi: 10.1007/s10661-014-4012-2.

[19] M. Amin and S. A. Romshoo, "Comparative assessment of soil erosion modelling approaches in a Himalayan watershed," Model. Earth Syst. Environ., vol. 5, no. 1, pp. 175–192, 2019, doi: 10.1007/s40808-018-0526-x.

[20] H. Abdo and J. Salloum, "Mapping the soil loss in Marqya basin: Syria using RUSLE model in GIS and RS techniques," Environ. Earth Sci., vol. 76, no. 3, p. 114, 2017, doi: 10.1007/s12665-017-6424-0.

[21] O. Djoukbala, M. Mazour, M. Hasbaia, and O. Benselama, "Estimating of water erosion in semiarid regions using RUSLE equation under GIS environment," Environ. Earth Sci., vol. 77, no. 9, p. 345, 2018, doi: 10.1007/s12665-018-7532-1.

[22] H. S. Gelagay and A. S. Minale, "Soil loss estimation using GIS and Remote sensing techniques: A case of Koga watershed, Northwestern Ethiopia," Int. Soil Water Conserv. Res., vol. 4, no. 2, pp. 126–136, 2016, doi: 10.1016/j.iswcr.2016.01.002.

[23] P. Rangsiwanichpong, S. Kazama, and L. Gunawardhana, "Assessment of sediment yield in Thailand using revised universal soil loss equation and geographic information system techniques," River Res. Appl., vol. 34, no. 9, pp. 1113–1122, 2018, doi: https://doi.org/10.1002/rra.3351.

[24] S. S. Biswas and P. Pani, "Estimation of soil erosion using RUSLE and GIS techniques: a case study of Barakar River basin, Jharkhand, India," Model. Earth Syst. Environ., vol. 1, no. 4, pp. 1–13, 2015, doi: 10.1007/s40808-015-0040-3.

[25] K. Balasubramani, M. Veena, K. Kumaraswamy, and V. Saravanabavan, "Estimation of soil erosion in a semi-arid watershed of Tamil Nadu (India) using revised universal soil loss equation (rusle) model through GIS," Model. Earth Syst. Environ., vol. 1, no. 3, pp. 1–17, 2015, doi: 10.1007/s40808-015-0015-4.

[26] L. Jiang, Z. Yao, Z. Liu, S. Wu, R. Wang, and L. Wang, "Estimation of soil erosion in some sections of Lower Jinsha River based on RUSLE," Nat. Hazards, vol. 76, no. 3, pp. 1831–1847, 2015, doi: 10.1007/s11069-014-1569-6.

[27] Q. Zhou, S. Yang, C. Zhao, M. Cai, and L. Ya, "A Soil Erosion Assessment of the Upper Mekong River in Yunnan Province, China," Mt. Res. Dev., vol. 34, no. 1, pp. 36–47, 2014, doi: 10.1659/MRD-JOURNAL-D-13-00027.1.

[28] S. Ullah, A. Ali, M. Iqbal, M. Javid, and M. Imran, "Geospatial assessment of soil erosion intensity and sediment yield: a case study of Potohar Region, Pakistan," Environ. Earth

Sci., vol. 77, no. 19, pp. 1–13, Oct. 2018, doi: 10.1007/S12665-018-7867-7/METRICS.

[29] H. Xie, Y. Zhang, Z. Wu, and T. Lv, "A bibliometric analysis on land degradation: Current status, development, and future directions," Land, vol. 9, no. 1, 2020, doi: 10.3390/LAND9010028.

[30] X. Chen, Z. Liang, Z. Zhang, and L. Zhang, "Effects of soil and water conservation measures on runoff and sediment yield in red soil slope farmland under natural rainfall," Sustain., vol. 12, no. 8, 2020, doi: 10.3390/SU12083417.

[31] I. C. Nicu, "Is overgrazing really influencing soil erosion?," Water (Switzerland), vol. 10, no. 8, pp. 1–16, 2018, doi: 10.3390/w10081077.

[32] R. U. Khan, T. Bannu, and T. Bannu, "Ethnobotanical Study of Food Value Flora of District Bannu Khyber Journal of Medicinal Plants Studies Ethnobotanical Study of Food Value Flora of District Bannu Khyber Pakhtunkhwa , Pakistan," no. June 2015, 2013.

[33] K. Pakhtunkhwa, M. Rooman, Y. Assad, S. Tabassum, S. Sultan, and S. Ayaz, "A cross-sectional survey of hard ticks and molecular characterization of Rhipicephalus microplus parasitizing domestic animals of," no. August, 2021, doi: 10.1371/journal.pone.0255138.

[34] T. S. Abdulkadir et al., "Quantitative analysis of soil erosion causative factors for susceptibility assessment in a complex watershed," Cogent Eng., vol. 6, no. 1, Jan. 2019, doi: 10.1080/23311916.2019.1594506.

[35] L. Tsegaye and R. Bharti, "Soil erosion and sediment yield assessment using RUSLE and GIS-based approach in Anjeb watershed, Northwest Ethiopia," SN Appl. Sci., vol. 3, no. 5, pp. 1–19, 2021, doi: 10.1007/s42452-021-04564-x.

[36] W. Maleika, "Inverse distance weighting method optimization in the process of digital terrain model creation based on data collected from a multibeam echosounder," Appl. Geomatics, vol. 12, no. 4, pp. 397–407, 2020, doi: 10.1007/s12518-020-00307-6.

[37] D. Liu, Q. Zhao, D. Fu, S. Guo, P. Liu, and Y. Zeng, "Comparison of spatial interpolation methods for the estimation of precipitation patterns at different time scales to improve the accuracy of discharge simulations," Hydrol. Res., vol. 51, no. 4, pp. 583–601, 2020, doi: 10.2166/NH.2020.146.

[38] N. Ejaz, M. Elhag, J. Bahrawi, L. Zhang, H. F. Gabriel, and K. U. Rahman, "Soil Erosion Modelling and Accumulation Using RUSLE and Remote Sensing Techniques: Case Study Wadi Baysh, Kingdom of Saudi Arabia," Sustain., vol. 15, no. 4, pp. 1–14, 2023, doi: 10.3390/su15043218.

[39] S. Y. Siswanto and M. I. S. Sule, "The Impact of slope steepness and land use type on soil properties in Cirandu Sub-Sub Catchment, Citarum Watershed," IOP Conf. Ser. Earth Environ. Sci., vol. 393, no. 1, 2019, doi: 10.1088/1755-1315/393/1/012059.

[40] I. A. N. D. Moore and G. J. Burch, "DIVISION S-6-SOIL AND WATER MANAGEMENT Physical Basis of the Length-slope Factor in the Universal Soil Loss Equation 1," Soil Conserv., vol. 50, no. 1986, pp. 1294–1298, 1986.

[41] I. D. Moore and G. J. Burch, "Modelling Erosion and Deposition: Topographic Effects.," Trans. Am. Soc. Agric. Eng., vol. 29, no. 6, pp. 1624–1630, 1986, doi: 10.13031/2013.30363.

[42] B. P. Ganasri and H. Ramesh, "Assessment of soil erosion by RUSLE model using remote sensing and GIS - A case study of Nethravathi Basin," Geosci. Front., vol. 7, no. 6, pp. 953–961, 2016, doi: 10.1016/j.gsf.2015.10.007.

[43] Y. Farhan and S. Nawaiseh, "Spatial assessment of soil erosion risk using RUSLE and GIS techniques," Environ. Earth Sci., vol. 74, no. 6, pp. 4649–4669, 2015, doi: 10.1007/s12665-015-4430-7.

[44] A. Y. Yesuph and A. B. Dagnew, "Soil erosion mapping and severity analysis based on RUSLE model and local perception in the Beshillo Catchment of the Blue Nile Basin, Ethiopia," Environ. Syst. Res., vol. 8, no. 1, pp. 1–21, 2019, doi: 10.1186/s40068-019-0145-1.

[45] C. M. Fayas, N. S. Abeysingha, K. G. S. Nirmanee, D. Samaratunga, and A. Mallawatantri, "Soil loss estimation using rusle model to prioritize erosion control in KELANI river basin in Sri Lanka," Int. Soil Water Conserv. Res., vol. 7, no. 2, pp. 130–137, 2019, doi: 10.1016/j.iswcr.2019.01.003.

[46] S. Batool, S. A. Shirazi, and S. A. Mahmood, "Research Article Appraisal of Soil Erosion through RUSLE Model and Hypsometry in Chakwal Watershed (Potwar-Pakistan)," 2021.